Discrete Implementation and Generalization of the Extended State Observer

Robert Miklosovic, Aaron Radke, and Zhiqiang Gao
Center for Advanced Control Technologies
Fenn College of Engineering, Cleveland State University
Cleveland, Ohio, USA
rmiklosovic@ieee.org

Abstract— **A brief review of developments in disturbance observers, leading up to the extended state observer (ESO), is first presented. Various digital implementations of the ESO are investigated and compared. The realization in current discrete estimator form evidently helps to maintain stable operation at low sampling rates. Digitization using zero order hold is derived symbolically to further improve accuracy while preserving the simplicity of single parameter tuning. Finally, the ESO is reformulated using a generalized disturbance model which provides a wider range of solutions for disturbance estimation problems. Application of the proposed algorithm is shown on a realistic motion control simulation platform with favorable results.**

Keywords—Estimator, Observer, Disturbance Observer, Extended State Observer, Unknown Input Observer, Output Feedback

I. INTRODUCTION

Observers extract real-time information of a plant's internal state from its input-output data. The observer usually presumes precise model information of the plant [1-8], since performance is largely based on its mathematical accuracy. Closed loop controllers require both types of information. Such presumptions, however, often make the method impractical in engineering applications, since the challenge for industry remains in constructing these models as part of the design process. Another level of complexity is added when gain scheduling and adaptive techniques are used to deal with nonlinearity and time variance, respectively.

To account for uncertainties in the real world, various techniques have been proposed [9-15] that solve the problem of model accuracy in reverse. This is done by modeling a plant P with an equivalent input disturbance d that includes unmodeled dynamics. An observer is then designed to estimate the disturbance in real time and provide feedback to cancel it. As a result, the augmented system reduces to the nominal model P_n at low frequencies, making it accurate.

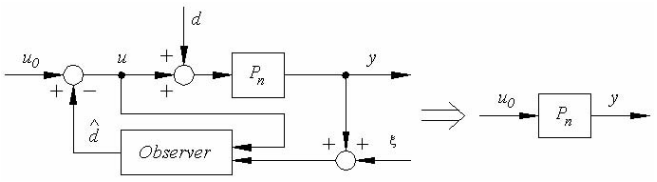

Figure 1. Disturbance Rejection

The most common of these techniques is the disturbance observer (DOB) framework [13, 16, 17]. It uses simple binomial Q-filters, allowing the observer to be tuned by a single bandwidth parameter. A model deliberately different from P is also suggested to facilitate design [17], but no guidelines are given other than it should be as simple as possible, cautioning stability and performance may be in danger. Another obstacle is that a separate observer must be designed to provide state feedback to the controller. In existing research, derivative approximates are used in this way but their affect on performance and stability has yet to be analyzed.

Another technique, referred to as the unknown input observer (UIO), estimates the states of both the plant and the disturbance by augmenting a linear design model with a linear disturbance model [6-12, 18]. Unlike the DOB, a controller and observer can be designed independently, like a Luenberger observer. However, it still relies on a good mathematical model and a design procedure to determine observer gains. In this regard, the extended state observer (ESO) is quite different. Originally proposed in the form of a nonlinear UIO [14] and later simplified to a linear version with one tuning parameter [15], the ESO combines the state and disturbance estimation power of a UIO with the tuning simplicity of a DOB.

One finds a decisive shift in the underlying design concept as well. The traditional observer is based on a linear time-invariant model that often describes a nonlinear time-varying process. Although the DOB and UIO reject input disturbances for such nominal plants, they leave the question of dynamic uncertainty mostly unanswered in direct form. The ESO, on the other hand, addresses both issues in one simple framework by formulating the simplest possible design model P_d for a large class of uncertain systems. P_d is selected to simplify controller and observer design, forcing P to behave like it at low frequencies rather than P_n. As a result, the effects of most plant dynamics and external disturbances are concentrated into a single unknown quantity. The ESO estimates this quantity along with derivatives of the output, giving way to the straightforward design of a high performance controller. Its practical usefulness is seen in a number of benchmark applications already implemented throughout industry [19-22] and even complex multivariable systems such as turbofan engines [23].

In this paper, enhancements are made to the ESO, both in formulation and in implementation. First, the ESO is discretized as a current discrete estimator to maintain stable operation at lower sampling rates, a major limiting factor in controls. Typical discretization methods, such as a predictive discrete estimator [6], generate at least one sample of delay, whereas a current discrete estimator removes this delay by adding a current time step update to the estimated state [6].

Supported by NASA grants NGT3-52387, NCC3-931, and NCC3-1081

Then, both zero order hold (ZOH) and first order hold (FOH) versions of all discrete matrices are determined symbolically to retain single parameter tuning. In the past, only Euler integration was used. Finally, the ESO is reformulated to incorporate a disturbance model of arbitrary order, thus allowing the amount of disturbance rejection to be specified for different types of disturbances. In the past, disturbances were restricted to first order.

A current discrete ESO is formulated and analyzed in Section II using symbolic Euler and ZOH methods. It is reformulated with multiple extended states for a system of arbitrary order in Section III using symbolic ZOH and FOH methods. Section IV provides a realistic simulation test of a motion control plant. Finally, concluding remarks are given in Section V.

II. Current Discrete Extended State Observer

For the sake of simplicity, consider a general second order plant where u and y are the input and output, respectively, and b is a constant.

$$\ddot{y} = g(y, \dot{y}, t) + w + bu \tag{1}$$

Combining the internal dynamics $g(y, \dot{y}, t)$ with an external disturbance w to form a generalized disturbance $f(y, \dot{y}, w, t)$, the system is rewritten as

$$\ddot{y} = f(y, \dot{y}, w, t) + bu\,. \tag{2}$$

A. Continuous Observer Design

An augmented state space model is constructed

$$\begin{aligned} \dot{x} &= Ax + Bu + E\dot{f} \\ y &= Cx + Du \end{aligned} \tag{3}$$

$$A = \begin{bmatrix} 0 & 1 & 0 \\ 0 & 0 & 1 \\ 0 & 0 & 0 \end{bmatrix}, \quad B = \begin{bmatrix} 0 \\ b \\ 0 \end{bmatrix}, \quad E = \begin{bmatrix} 0 \\ 0 \\ 1 \end{bmatrix}$$
$$C = \begin{bmatrix} 1 & 0 & 0 \end{bmatrix}, \quad D = \begin{bmatrix} 0 \end{bmatrix}$$

where $x = [y, \dot{y}, f]^T$ includes the disturbance to be estimated.

Next, an observer is created from the state space model.

$$\begin{aligned} \dot{\hat{x}} &= A\hat{x} + Bu + L(y - \hat{y}) \\ \hat{y} &= C\hat{x} + Du \end{aligned} \tag{4}$$

Note that $\dot{f}$ is ignored in (4) since it is unknown and is estimated by the correction term. The observer is rewritten to output the state

$$\begin{aligned} \dot{\hat{x}} &= [A - LC]\hat{x} + [B - LD,\ L]u_c \\ y_c &= \hat{x} \end{aligned} \tag{5}$$

where $u_c = [u, y]^T$ is the combined input and y_c is the output. It is then decomposed into individual state equations for the purpose of implementation. For the sake of simplicity, the observer gain vector L is determined by placing the poles of the characteristic equation in one location.

$$\lambda(s) = \left| sI - (A - LC) \right| = (s + \omega_o)^3 \tag{6}$$
$$L = \left[3\omega_o,\ 3\omega_o^2,\ \omega_o^3\right]^T$$

B. Discrete Estimator Design

The state space model in (3) is first discretized by applying Euler, ZOH, or FOH.

$$\begin{aligned} \hat{x}(k+1) &= \Phi\hat{x}(k) + \Gamma u(k) \\ \hat{y}(k) &= H\hat{x}(k) + J\,u(k) \end{aligned} \tag{7}$$

A discrete observer is created from this model.

$$\begin{aligned} \hat{x}(k+1) &= \Phi\hat{x}(k) + \Gamma u(k) + L_p(y(k) - \hat{y}(k)) \\ \hat{y}(k) &= H\hat{x}(k) + J\,u(k) \end{aligned} \tag{8}$$

This is known as a predictive discrete estimator [6] because the current estimation error $y(k) - \hat{y}(k)$ is used to predict the next state estimate $\hat{x}(k+1)$. However, by defining the predictive estimator gain vector as

$$L_p = \Phi L_c\,, \tag{9}$$

the estimated state reduces to

$$\hat{x}(k+1) = \Phi\bar{x}(k) + \Gamma u(k) \tag{10}$$

where the new state includes a current time step update, giving it less time delay.

$$\bar{x}(k) = \hat{x}(k) + L_c(y(k) - \hat{y}(k)) \tag{11}$$

This is referred to as a current discrete estimator [6]. When the sampling rate is low, this could play a significant role in enhancing the stability of a closed loop system. A block diagram is illustrated below.

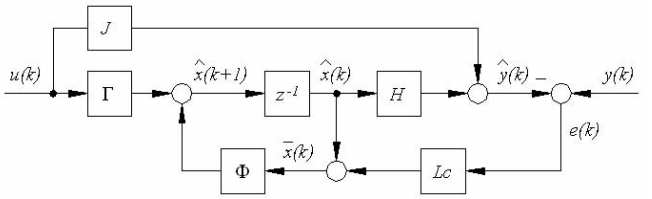

Figure 2. Current Discrete Estimator

The estimator is then rewritten to output the new state

$$\begin{aligned} \hat{x}(k+1) &= [\Phi - L_p H]\hat{x}(k) + [\Gamma - L_p J,\ L_p]u_d(k) \\ y_d(k) &= [I - L_c H]\hat{x}(k) + [-L_c J,\ L_c]u_d(k) \end{aligned} \tag{12}$$

where $u_d(k) = [u(k), y(k)]^T$ is the combined input and y_d is the output. The only difference for the predictive estimator is that $y_d(k) = \hat{x}(k)$. For the sake of simplicity, the current estimator gain vector L_c is determined by placing the poles of the discrete characteristic equation in one location.

$$\lambda(z) = \left| zI - (\Phi - \Phi L_c H) \right| = (z - \beta)^3 \tag{13}$$

The relation between the discrete estimator poles and the continuous observer poles is given as

$$\beta = e^{-\omega_o T}\,. \tag{14}$$

Applying Euler to (3) and solving (13) for L_c yields

$$\Phi = \begin{bmatrix} 1 & T & 0 \\ 0 & 1 & T \\ 0 & 0 & 1 \end{bmatrix}, \quad \Gamma = \begin{bmatrix} 0 \\ b \\ 0 \end{bmatrix}, \quad L_c = \begin{bmatrix} 1-\beta^3 \\ (2-3\beta+\beta^3)\frac{1}{T} \\ (1-\beta)^3 \frac{1}{T^2} \end{bmatrix}. \quad (15)$$
$$H = \begin{bmatrix} 1 & 0 & 0 \end{bmatrix}, \quad J = \begin{bmatrix} 0 \end{bmatrix}$$

where T is the discrete sample time. However, note that $[.]^T$ is denoted as the matrix transpose. In the past, the ESO was implemented by integrating each state equation in (4) using Euler [14, 15, 19-23]. The problem with this method is that it produces the same matrices as (15) except for $L_p = TL$, making the observer unstable at relatively low sample rates. Yet in cases where L is a nonlinear function, this may be the only way of discrete implementation. For the sake of further discussion, it is referred to as the Euler approximation.

Applying ZOH

$$\Phi = e^{AT} \quad \Rightarrow \quad \sum_{k=0}^{\infty} \frac{A^k T^k}{(k)!}$$
$$\Gamma = \int_0^T e^{A\tau} d\tau \, B \quad \Rightarrow \quad \sum_{k=0}^{\infty} \frac{A^k T^{k+1}}{(k+1)!} B \quad (16)$$
$$H = C, \quad J = 0$$

to (3) produces a more accurate estimation than Euler.

$$\Phi = \begin{bmatrix} 1 & T & \frac{T^2}{2} \\ 0 & 1 & T \\ 0 & 0 & 1 \end{bmatrix}, \; \Gamma = \begin{bmatrix} bT \\ b \\ 0 \end{bmatrix}, \; L_c = \begin{bmatrix} 1-\beta^3 \\ (1-\beta)^2(1+\beta)\frac{3}{2T} \\ (1-\beta)^3 \frac{1}{T^2} \end{bmatrix} \quad (17)$$
$$H = \begin{bmatrix} 1 & 0 & 0 \end{bmatrix}, \; J = \begin{bmatrix} 0 \end{bmatrix}$$

Note that it becomes an $\alpha - \beta - \gamma$ filter when $b=0$ [24].

C. Simulation and Analysis

The ESO is first applied in open loop to a simple plant

$$\ddot{y} = 50\dot{y} + 500u + 100w \quad (18)$$

where w is a 2.5Hz square wave starting at 0.3 sec. and u is a trapezoidal profile that lasts 0.125 sec. The estimator parameters are ω_o =300 and T = 0.005. A tracking error plot is shown below that compares the predictive and current discrete methods using both Euler and ZOH.

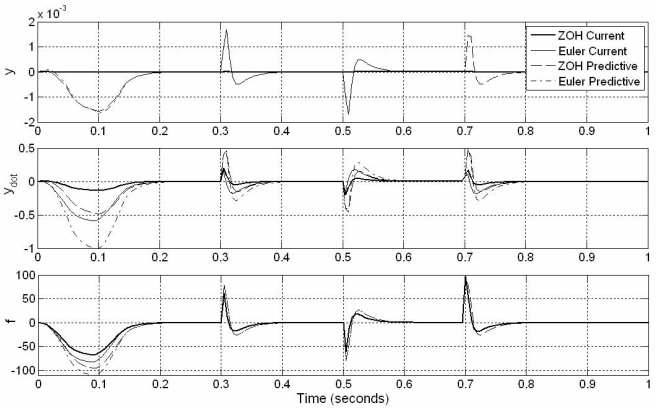

Figure 3. Open Loop Tracking Error

The transient and steady state parts of each trajectory are evaluated using integral absolute error and then summarized in the following table.

TABLE I. OPEN LOOP TRACKING ERRORS

Discretization Method	Transient Integral Absolute Error		
	y	y'	f
ZOH Current	1.49E-6	12E-3	5.90
Euler Current	1.51E-6	51E-3	7.16
ZOH Predictive	136E-6	41E-3	8.41
Euler Predictive	134E-6	87E-3	9.66
Discretization Method	**Steady State Integral Absolute Error**		
	y	y'	f
ZOH Current	0.10E-5	9E-3	2.83
Euler Current	0.10E-5	20E-3	2.83
ZOH Predictive	9.55E-5	30E-3	4.32
Euler Predictive	9.55E-5	40E-3	4.32

When the step size T = 0.005, the Euler approximation becomes unstable and therefore was not shown. However, the four methods shown use discrete pole placement and do not become unstable until T = 0.066. From the table, the second most important option appears to be the current discrete method for tracking accuracy. The table also shows that ZOH is better than Euler and, interestingly, dominant in estimating transient velocity.

Next, the ESO is applied in closed loop to (18) and to a more complex simulation of an actual servo-motor.

$$V_m = 80(75u - .075I_a), \quad |V_m| < 160, \quad |u| < 8$$
$$\dot{I}_a = 2500\,(V_m - .4I_a - 1.2\dot{y}) \quad (19)$$
$$\ddot{y} = 11.1(100w + 1.5I_a)$$

The closed loop method is outlined in Section IV. With ω_c =30 and ω_o =300, the sample period is increased to the point of instability and then tabulated below.

TABLE II. MAXIMUM CLOSED LOOP STEPSIZE

Discretization Method	Simple Plant (18)	Servo-motor (19)
Euler Approximation	26E-4	30E-4
Euler Predictive	37E-4	57E-4
Euler Current	47E-4	68E-4
ZOH Predictive	85E-4	140E-4
ZOH Current	150E-4	300E-4

The results show that the most important option for low sampling time requirements is ZOH, followed by the current discrete method. In this regard, the current discrete ESO with ZOH appears to be six to ten times better than the Euler approximation used in previous literature. The servo system in Section IV was also simulated, resulting in an improvement of 5.3 times. In summary, the current discrete ESO with ZOH should be used for improved tracking accuracy as well as closed loop stability.

III. GENERALIZED EXTENDED STATE OBSERVER

Although a second order example was used in Section II, (4) through (14) and (16) are applicable to a plant of arbitrary

order with any number of extended states. For example, a class of general n^{th} order plants similar to (1) is represented as

$$y^{(n)} = g(y,\cdots,y^{(n-1)},t) + w + bu \tag{20}$$

where $y^{(n)}$ denotes the n^{th} derivative of the output and $g(y,\cdots,y^{(n-1)},t)$ represents the internal dynamics. Two critical parameters are relative order n and high frequency gain b [25]. Combining the unknowns into one generalized disturbance $f(y,\cdots,y^{(n-1)},w,t)$ results in

$$y^{(n)} = f(y,\cdots,y^{(n-1)},w,t) + bu\,. \tag{21}$$

Note that when represented with an equivalent input disturbance $d=f/b$, the design model becomes

$$P_d(s) = b/s^n\,. \tag{22}$$

As a signal, the type of disturbance can be characterized similar that of system type in a classical control. This specification is outlined in [7] as the degree of a polynomial that approximates a signal, which directly relates to the number of times it is differentiated before reaching zero. Sometimes disturbances are represented by a set of cascaded integrators $1/s^h$ with unknown input [6, 8, 10-12, 18]. Under this assumption, the plant is represented by two sets of cascaded integrators; one for the design model and another for the disturbance model.

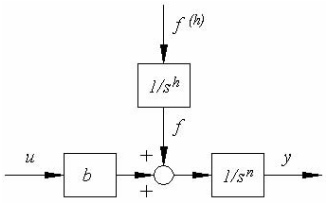

Figure 4. Canonical Form with Distrubance Model

It will also be shown that this assumption leads to an estimated disturbance equivalent to that of a DOB.

In (3), previous ESO design [14, 15, 19-23], and in [6, 17-18] disturbances are considered to be piece-wise constant with $h = 1$ or a series of steps. Now an ESO with $h = 1, 2, 3$ can respectively track a square, triangular, or parabolic disturbance. A sinusoid is a different matter because it is infinitely differentiable. However, increasing h increases the degree of the polynomial and improves tracking of a sinusoid or any time varying disturbance. An ESO with h extended states for a relative n^{th} order plant is denoted as an $ESO_{n,h}$.

A. Continuous Observer Design

The new form is represented in state space

$$\begin{aligned} \dot{x} &= Ax + Bu + Ef^{(h)} \\ y &= Cx + Du \end{aligned} \tag{23}$$

where the state includes the disturbance f and its derivatives to be estimated.

$$\begin{aligned} x &= [x_1,\cdots,x_n,x_{n+1},\cdots,x_{n+h}]^T \\ &= [y^{(0)},\cdots,y^{(n-1)},f^{(0)},\cdots,f^{(h-1)}]^T \end{aligned} \tag{24}$$

Since the new form consists of cascaded integrators, the A matrix simplifies to an $n+h$ square matrix with ones on the super diagonal. Each element of A is defined as

$$a_{i,j} = \begin{cases} 1, i = j-1 \\ 0, otherwise \end{cases}. \tag{25}$$

Since the input is added after n-integrators, the first state is defined as the output, and the derivative of the last state is $f^{(h)}$, the other matrices become

$$B = [0_{n-1} \quad b \quad 0_h]^T,\ C = [1 \quad 0_{n+h-1}],\ E = [0_{n+h-1} \quad 1]^T \tag{26}$$

where 0_h represents a $1\times h$ zero vector and $D = 0$.

For the sake of simplicity, the observer gain vector is determined by placing all of the poles of the characteristic equation in one location.

$$\lambda(s) = |sI - (A - LC)| = (s + \omega_o)^{n+h} \tag{27}$$

As a result, each element in L becomes

$$l_i = c_{n+h,i}\omega_o^i, \quad i = 1,2,\cdots,n+h \tag{28}$$

where the binomial coefficients are $c_{i,j} = \binom{i}{j} = \frac{i!}{j!(i-j)!}$.

The ESO can also be represented in filter form

$$\begin{aligned} \hat{y}^{(i)} &= s^i[Q_y y + (1-Q_y)P_d u], \quad i = 0,\cdots,n-1 \\ \hat{f}^{(j)} &= s^j[bQ_f(P_d^{-1}y - u)], \quad j = 0,\cdots,h-1 \end{aligned} \tag{29}$$

where binomial filters

$$Q_y(s) = \frac{\beta_{n+h,\,n+h-i-1}(s)}{\beta_{n+h,\,n+h}(s)}, \quad Q_f(s) = \frac{\beta_{n+h,\,h-j-1}(s)}{\beta_{n+h,\,n+h}(s)} \tag{30}$$

consist of numerator and denominator polynomials that are functions of a single tuning parameter $\omega_o = 1/\tau$.

$$\beta_{i,j}(s) = 1 + \sum_{r=1}^{j} c_{ir}(\tau s)^r \tag{31}$$

This form shows that additional extended states raise observer order, $n+h$, and increase the slope of the cutoff frequency. It also shows that the estimated disturbance is equivalent to a DOB, i.e. a filtered version of the actual f.

$$\hat{f} = bQ_f(P_d^{-1}y - u) \tag{32}$$

B. Discrete Estimator Design

Applying ZOH to (23) using (16) produces an $n+h$ square Φ matrix where each element is defined as

$$\phi_{i,j} = \begin{cases} \gamma_{j-i}, & i \le j \\ 0, otherwise \end{cases} \tag{33}$$

for $\gamma_k = T^k/k!$. The Γ matrix reduces to

$$\Gamma = [b\gamma_n \quad \cdots \quad b\gamma_1 \quad 0_h]^T. \tag{34}$$

If FOH is preferred, the only change is in the Γ and J matrices, which become

$$\Gamma = \begin{bmatrix} \dfrac{(2^{n+1}-2)}{n+1} b\gamma_n & \cdots & \dfrac{2}{2} b\gamma_1 & 0_h \end{bmatrix}^T \qquad (35)$$
$$J = \begin{bmatrix} \dfrac{b\gamma_n}{n+1} & \cdots & \dfrac{b\gamma_1}{2} & 0_h \end{bmatrix}^T$$

For the sake of simplicity, the current estimator gain vector L_c is determined by placing the poles of the discrete characteristic equation in one location.

$$\lambda(z) = \left| zI - (\Phi - \Phi L_c H) \right| = (z-\beta)^{n+h} \qquad (36)$$

As a result, the current estimator gain vector is listed in the table as a function of $n+h$. A current discrete ESO with h extended states for a relative n^{th} order plant is denoted as a $CDESO_{n,h}$.

TABLE III. CDESO ESTIMATOR GAINS FOR ZOH AND FOH

$n+h$	L_c
1	$\left[1-\beta\right]^T$
2	$\left[1-\beta^2, (1-\beta)^2 \frac{1}{T}\right]^T$
3	$\left[1-\beta^3, (1-\beta)^2(1+\beta)\frac{3}{2T}, (1-\beta)^3 \frac{1}{T^2}\right]^T$
4	$\left[1-\beta^4, (1-\beta)^2(11+\beta(14+11\beta))\frac{1}{6T}, (1-\beta)^3(1+\beta)\frac{2}{T^2}, (1-\beta)^4 \frac{1}{T^3}\right]^T$
5	$\left[1-\beta^5, (1-\beta)^2(1+\beta)(5+\beta(2+5\beta))\frac{5}{12T}, (1-\beta)^3(7+\beta(10+7\beta))\frac{5}{12T^2}, (1-\beta)^4(1+\beta)\frac{5}{2T^3}, (1-\beta)^5 \frac{1}{T^4}\right]^T$

IV. DESIGN EXAMPLE

A simulation of an industrial motion control test bed is used to demonstrate the control design procedure and its simplicity, resulting performance, and overall effectiveness in the absence of a simulation model. The servo amplifier, motor, and drive train are modeled with a resonant load as

$$\begin{aligned} V_m &= 4(V_c - 2.05 I_a), \quad |V_c| < 4.5, \quad |V_m| < 10 \\ \dot{I}_a &= 2500(V_m - 4I_a - .2\dot{x}_m), \quad |I_a| < 1 \\ T_m &= .5 I_a - T_d - T_l \\ T_l &= .0005(\dot{x}_m - 4\dot{x}_l) + .0001(x_m - 4x_l) \\ \ddot{x}_m &= 2500 T_m \\ \ddot{x}_l &= 175 T_l \end{aligned} \qquad (37)$$

where V_c, x_l, and T_d are the control input voltage, output load position, and torque disturbance, respectively. Backlash of a ±0.31μm/sec. dead-bandwidth on $\dot{x}$ is also applied.

The control design method using the ESO is fairly straight forward with only a few physical intuitions. In the most basic sense, a servo motor can be considered as a double integrator.

$$\frac{x_l(s)}{V_c(s)} \approx \frac{b_m}{s^2}. \qquad (38)$$

It is put into the new canonical form where $f(t)$ represents any of the discrepancies or dynamics not modeled in (38).

$$\ddot{x}_l(t) = f(t) + b_m V_c(t) \qquad (39)$$

First, a $CDESO_{2,h}$ is used to estimate $x_l(t)$, $\dot{x}_l(t)$, and $f(t)$ in discrete time. Then the estimated disturbance is fed back to cancel itself

$$V_c(k) = \frac{u_0(k) - \hat{f}(k)}{b_m} \qquad (40)$$

which reduces the system to a double integrator, $\ddot{x}_l(t) \approx u_0(t)$. Finally, a parameterized control law is used to control the augmented system where $r(k)$ is a reference motion profile.

$$u_0(k) = \omega_c^2 (r(k) - \hat{x}_l(k)) - 2\omega_c \hat{\dot{x}}_l(k) \qquad (41)$$

The observer and control laws in (40) and (41) are selected with a sample rate of 10 kHz to control the motion system's model in (37). The gain b_m = 25 is crudely estimated as the initial acceleration from a step response. Disturbance rejection was tested by applying various torque disturbances at time t = 1 second and 0.1% white noise is injected into the output. Keeping the control signal within ±4.5V and its noise level within ±100mV, ω_c and ω_o were increased to 50 and 150, respectively. The results for a type 1 square, type 2 triangular, and type ∞ sinusoidal torque disturbance are shown in the following figures.

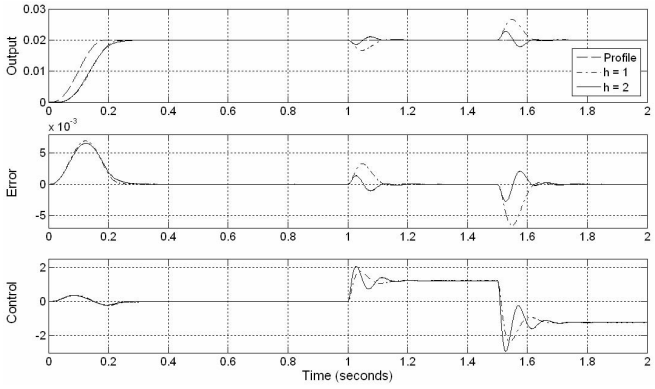

Figure 5. Response to a Square Torque Disturbance

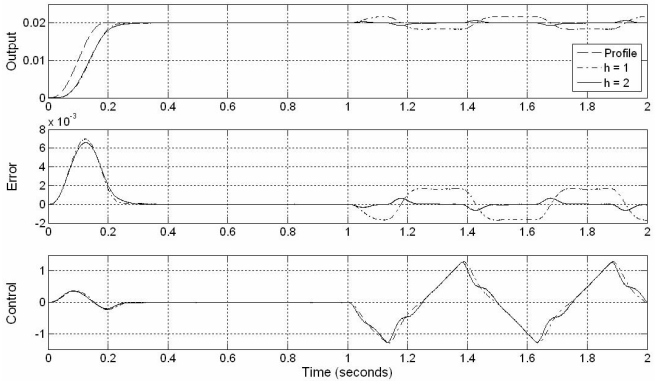

Figure 6. Response to a Triangular Torque Disturbance

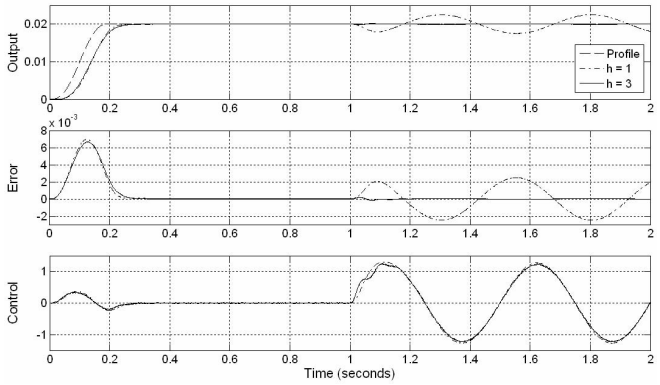

Figure 7. Response to a Sinusoidal Torque Disturbance

Robustness was tested by increasing the load by a factor of nearly 8. There was no noticeable difference.

The results show that two extended states reduce the error compared to one extended state. In Fig. 6, two extended states drive to zero the error created by type 2 disturbances. Although a sinusoidal disturbance is infinitely differentiable, three extended states significantly reduce the steady state error in Fig. 7.

V. Concluding Remarks

Various discrete implementations of the extended state observer are studied and compared in this paper. It is shown that the current discrete formulation is superior to the predictive one in reducing the delay associated with the sampling process. It is also demonstrated that the ZOH implementation improves estimation accuracy and stability without additional complexity to the user. To facilitate the ESO implementation for practitioners, the algorithm is derived symbolically with a single tuning parameter, i.e. the bandwidth of the observer. Another significant development is the generalization of the ESO for various types of systems and disturbances. Finally, a filter version shows that the estimated disturbance is equivalent to the DOB structure. Unlike the DOB, however, the ESO estimates suitable derivatives of the output, allowing for a straightforward controller design. The motion control problem is complex with many uncertainties, yet preliminary results show that this observer can achieve high performance over a wide range of system dynamics while remaining easy to use.

References

[1] Kalman, Rudolph, and Emil, "A new approach to linear filtering and prediction problems," *Transactions of the ASME–Journal of Basic Engineering*, vol. 82, no. Series D, pp. 35–45, 1960.

[2] D. Luenberger, "Observers for multivariable systems," *IEEE Transactions on Automatic Control*, vol. 11, no. 2, pp. 190–197, 1966.

[3] J. C. Doyle and G. Stein, "Multivariable feedback design: Concepts for a classical/modern synthesis," *Automatic Control, IEEE Transactions on*, vol. 26, no. 1, pp. 4 –16, 1981.

[4] B. Friedland, *The Control Handbook*. CRC Press, IEEE Press, 1996, ch. Observers, pp. 607–618.

[5] C.-T. Chen, *Linear System Theory and Design (Oxford Series in Electrical and Computer Engineering),* 3rd ed. Oxford University Press, August 1998.

[6] G.F. Franklin, J.D. Powell, and M. Workman, *Digital Control of Dynamic Systems*, 3rd ed., Menlo Park, CA: Addison Wesley Longman, Inc., 1998, pp. 328-337.

[7] G.F. Franklin, J.D. Powell, and A. Emami-Naeni, *Feedback Control of Dynamic Systems*, 4th ed., Upper Saddle River, NJ: Prentice-Hall, Inc., 2002, pp. 239-242, 601-604.

[8] A. Radke and Z. Gao, "A survey of state and disturbance observers for practitioners," Proc. of the American Control Conference, June 14-16 2006.

[9] G. Basile and G. Marro, "On the observability of linear, time-invariant systems with unknown inputs," *Journal of Optimization theory and applications*, vol. 2, no. 6, pp. 410–415, 1969.

[10] C. Johnson, "Accommodation of external disturbances in linear regulator and servomechanism problems," *IEEE Transactions on Automatic Control*, vol. AC-16, no. 6, pp. 635–644, December 1971.

[11] G. H. Hostetter and J. Meditch, "On the generalization of observers to systems with unmeasurable, unknown inputs," *Automatica*, vol. 9, pp. 721–724, 1973.

[12] C. Johnson, "Theory of disturbance-accommodating controllers," *Control and Dynamic Systems*, vol. 12, pp. 387–489, 1976.

[13] T. Umeno and Y. Hori, "Robust speed control of dc servomotors using modern two degrees-of-freedom controller design," *IEEE Transactions on Industrial Electronics*, vol. 38, no. 5, pp. 363–368, October 1991.

[14] J. Han, "Nonlinear Design Methods for Control Systems", Proc. 14th IFAC World Congress, 1999.

[15] Z. Gao, "Scaling and bandwidth-parameterization based controller tuning," American Control Conference, pp. 4989 – 4996, June 2003.

[16] Y. Hori and K. Shimura, "Position/force control of muli-axis robot manipulator based on the tdof robust servo controller for each joint," Proc. of the American Control Conference ACC/WM9, vol. 1, pp. 753–757, 1992.

[17] E. Schrijver and J. van Dijk, "Disturbance observers for rigid mechanical systems: Equivalence, stability, and design," *Journal of Dynamic Systems, Measurement, and Control*, vol. 124, no. 4, pp. 539–548, 2002.

[18] J. B. Burl, *Linear Optimal Control: H_2 and H_∞ methods*. Addison Wesley, 1999.

[19] Z. Gao and S. Hu, "A novel motion control design approach based on active disturbance rejection," Proc. of the 40th IEEE conference on Decision and Control, p. 4974, December 2001.

[20] Y. Hou, Z. Gao, F. Jiang, and B. T. Boulter, "Active disturbance rejection control for web tension regulation," IEEE Conference on Decision and Control, 2001.

[21] B. Sun, "Dsp-based advanced control algorithms for a dc-dc power converter," Master's thesis, Cleveland State University, June 2003.

[22] R. Kotina, Z. Gao, and A. J. van den Bogert, "Modeling and control of human postural sway," XXth Congress of the International Society of Biomechanics, Cleveland, Ohio, July 31 - August 5, 2005.

[23] R. Miklosovic and Z. Gao, "A dynamic decoupling method for controlling high performance turbofan engines," Proc. of the 16th IFAC World Congress, July 4-8, 2005.

[24] D. Tenne and T. Singh, "Characterizing performance of $\alpha - \beta - \gamma$ filters," *IEEE Transactions on Aerospace and Elecctronic Systems*, vol. 38, no. 3, pp. 1072–1087, July 2002.

[25] R. Miklosovic and Z. Gao, "A robust two-degree-of-freedom control design technique and its practical application", Proc. of the IEEE Industrial Application Society World Conference, Oct. 3-7, 2004.